

# TRANSPORT PROPERTIES OF THERMAL PLASMA CONTAINING FLUORO-NITRILE (C<sub>4</sub>F<sub>7</sub>N)-BASED GAS MIXTURES

V.R.T. NARAYANAN<sup>a,\*</sup>, CH. RÜMLER<sup>b</sup>, M. GNYBIDA<sup>a</sup>, P. SLAVÍČEK<sup>c</sup>

<sup>a</sup> Eaton European Innovation Center, Bořivojova 2380, 252 63 Roztoky, Czech Republic

<sup>b</sup> Eaton Industries GmbH, Hein-Moeller-Straße 7-11, 53115 Bonn, Germany

<sup>c</sup> Department of Physical Chemistry, University of Chemistry and Technology, Technická 5, 166 28 Prague, Czech Republic

\* VenkatRNarayanan@Eaton.com

**Abstract.** Gas mixtures containing fluoro-nitriles C<sub>4</sub>F<sub>7</sub>N or fluoro-ketones C<sub>5</sub>F<sub>10</sub>O as minority components (<20%) have been identified as promising alternatives to SF<sub>6</sub> in medium voltage gas-insulated switchgear (GIS) applications, because of their low Global Warming Potential together with their dielectric strength values being comparable to SF<sub>6</sub>. The buffer gases in such fluoro-nitrile or fluoro-ketone based gas mixtures are usually N<sub>2</sub>, O<sub>2</sub>, CO<sub>2</sub>, or air. In this contribution, we provide calculation results of transport properties, assuming local thermodynamic equilibrium (LTE), of thermal plasma containing following gas mixtures: C<sub>4</sub>F<sub>7</sub>N – CO<sub>2</sub> and C<sub>4</sub>F<sub>7</sub>N – CO<sub>2</sub> – O<sub>2</sub>. The modifications in the thermodynamic and transport properties upon the addition of oxygen to the C<sub>4</sub>F<sub>7</sub>N – CO<sub>2</sub> mixtures in the temperature range 300 K–30 kK at 1 bar are provided and discussed. These properties have been utilized to calculate the plasma temperature profile for a free-burning arc in a companion paper.

**Keywords:** Fluoro-nitrile, thermal plasma, transport properties, SF<sub>6</sub> alternative.

## 1. Introduction

In the decades following the Kyoto Protocol (1997), there has been an active industry-wide interest in analyzing possible replacements to SF<sub>6</sub> in high voltage gas-insulated switchgear applications with voltage ratings greater than 52 kV [1]. In the last 5 years, focus has been oriented towards replacing SF<sub>6</sub> in secondary distribution networks possessing medium voltage gas-insulated switchgear with substantially lower voltage ratings  $\leq 24$  kV. Unlike the high pressures greater than 5 bar observed in high voltage switchgear designs, typical pressurization level in medium voltage GIS equipment is close to atmospheric. Nonetheless, owing to the high boiling points (at 1 bar) of the promising main alternatives – fluoro-ketones (C<sub>5</sub>F<sub>10</sub>O, 27°C) and fluoro-nitriles (C<sub>4</sub>F<sub>7</sub>N, –4.7°C), suitable buffer gases like air or CO<sub>2</sub> for example, are added to prevent liquefaction at temperatures lower than –30°C. The main alternative to SF<sub>6</sub> gas has a mole fraction of less than 20%, so that the overall mixture possesses a significantly lower Global Warming Potential (GWP) compared to SF<sub>6</sub>. Furthermore, depending on the specific application, SF<sub>6</sub> or the proposed alternative gas mixtures could either be utilized as: (a) an insulation medium and/or, (b) a nominal current switching medium. During switching high temperature thermal plasma with temperatures in the order of 10 kK is generated and thermodynamic and transport properties of the arc plasma are needed to accurately model its behavior within the switchgear geometry. Fluoro-nitrile based mixtures are in the

focus of this contribution. Here CO<sub>2</sub> has been identified as a suitable buffer gas in the literature and O<sub>2</sub> is added to significantly reduce the generation of carbon monoxide (CO).

Elements	N, O, C, F
Polyatomic species	C <sub>2</sub> N <sub>2</sub> , C <sub>2</sub> N, CN <sub>2</sub> , NF <sub>2</sub> , NF <sub>3</sub> , N <sub>2</sub> F <sub>2</sub> , N <sub>2</sub> F <sub>4</sub> , CF <sub>2</sub> , CF <sub>3</sub> , CF <sub>4</sub> , C <sub>2</sub> F, C <sub>2</sub> F <sub>2</sub> , C <sub>2</sub> F <sub>3</sub> , C <sub>2</sub> F <sub>4</sub> , C <sub>2</sub> F <sub>5</sub> , C <sub>2</sub> F <sub>6</sub> , C <sub>3</sub> F <sub>6</sub> , C <sub>3</sub> F <sub>5</sub> N, C <sub>3</sub> F <sub>4</sub> N, C <sub>2</sub> F <sub>3</sub> N, CFN, C <sub>2</sub> FN, C <sub>4</sub> F <sub>7</sub> N, N <sub>2</sub> O, NO <sub>2</sub> , NOF, NFO <sub>2</sub> , NFO <sub>3</sub> , NOF <sub>3</sub> , F <sub>2</sub> O, F <sub>2</sub> O <sub>2</sub> , CFO, COF <sub>2</sub> , C <sub>2</sub> F <sub>4</sub> O, C <sub>3</sub> O <sub>2</sub> , C <sub>2</sub> O, CO <sub>2</sub> , O <sub>3</sub>
Diatomic species	F <sub>2</sub> , N <sub>2</sub> , N <sub>2</sub> <sup>+</sup> , CN, CN <sup>+</sup> , NF, CF, NO, NO <sup>+</sup> , CO, O <sub>2</sub> , O <sub>2</sub> <sup>+</sup>
Monatomic species and ions	F, F <sup>+</sup> , F <sup>2+</sup> , F <sup>3+</sup> , N, N <sup>+</sup> , N <sup>2+</sup> , N <sup>3+</sup> , C, C <sup>+</sup> , C <sup>2+</sup> , C <sup>3+</sup> , O, O <sup>+</sup> , O <sup>2+</sup> , O <sup>3+</sup> , e <sup>-</sup>

Table 1. List of species used in species composition calculations.

In this work, we calculate the relevant properties for the fluoro-nitrile-based C<sub>4</sub>F<sub>7</sub>N – CO<sub>2</sub> – O<sub>2</sub> mixtures for the temperature range 300 K–30 kK and pressure of 1 bar, with maximum mole fractions of C<sub>4</sub>F<sub>7</sub>N and O<sub>2</sub> being 20%. We have independently validated our results for 10% and 20% C<sub>4</sub>F<sub>7</sub>N mixed with CO<sub>2</sub> mixtures at 5 atm for the different properties of interest and have observed very good agreement with recently published data [2], except for dynamic vis-

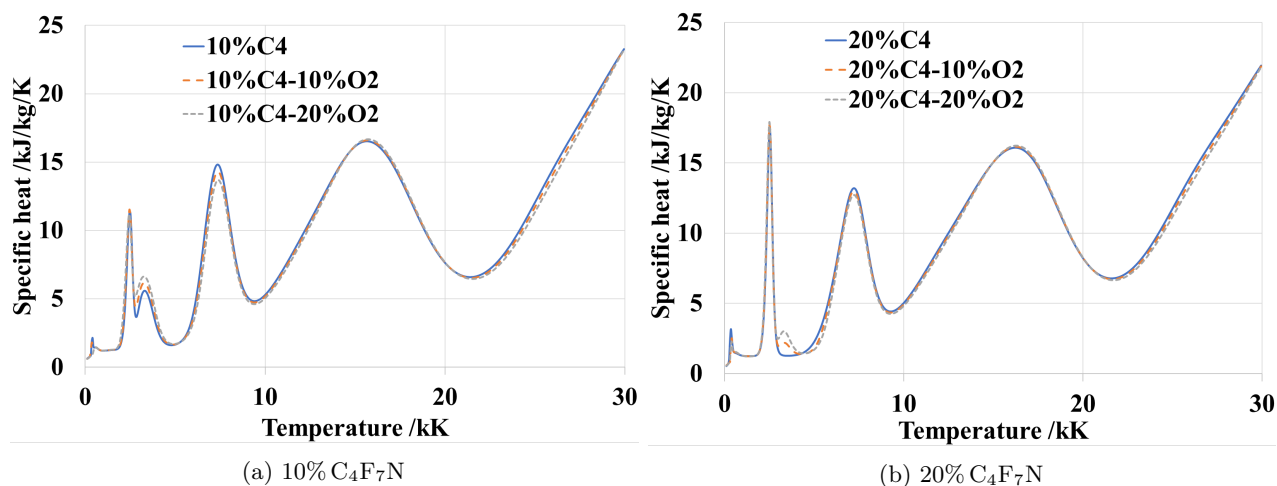


Figure 1. Specific heat values for different  $C_4F_7N$  ( $C_4$ ) mixtures at 1 bar.

cosity. These validation results are not provided here since the properties results at high pressures ( $>1$  atm) are beyond the scope of current work.

## 2. Species composition

The list of species considered for the species composition calculations have been provided in Table 1. The following species were omitted in this work, to facilitate a direct comparison with recent results from the literature [2]:  $C_4F_6$ ,  $C_3F_8$ ,  $C_3F_7$ ,  $C_3F_4$ ,  $C_2$ ,  $C_3$ ,  $C_4$ ,  $COF_4$ ,  $CO^+$ . Nonetheless, in a future work, results including these species will be considered, since the species composition and hence the properties at temperatures lower than 5 kK are expected to be different in the presence of the omitted species. Also, the condensed species (graphite) has not been included in the species list and consequently, the species composition is not expected to be accurate at temperatures lower than 2 kK. This discrepancy will also be addressed in a future work.

The molecular spectroscopic data – moments of inertia, vibrational frequencies, and the corresponding degeneracies – are necessary to calculate the internal partition functions and finally, the equilibrium composition of gas mixtures through the minimization of Gibbs free energy. However, such data is unavailable in the literature for several complex polyatomic species included in this current work. For these species we have utilized composite methods: CBS–QB3 by Petersson [3] and G4 method by Curtiss (B3LYP/aug-cc-pVTZ basis) [4] to evaluate the relevant molecular data. For the sake of brevity, the species composition results for the  $C_4F_7N - CO_2 - O_2$  mixtures will not be provided. With all the afore mentioned input data, the computationally efficient algorithm of Godin and Trepanier [5] was employed to determine the equilibrium composition.

## 3. Thermodynamic properties

Once the species composition has been obtained, the total enthalpy and the specific heat at constant pressure ( $C_p$ ) of the gas mixtures can be calculated through the calculation of mass density and partial derivatives of the total partition functions with respect to temperature. The variation of specific heat with temperature for 10% and 20%  $C_4F_7N$ -based mixtures are depicted in figure 1. The peaks below 1 kK are observed to have contributions from bigger polyatomic species -  $C_2F_6$  and  $CF_4$ . The peaks at 2.5 kK, 3.5 kK, and 7 kK are owing to the contributions from dissociation of  $COF_2$ ,  $CO_2$  and  $CO$  respectively, while the peak at 16 kK pertains to the contributions from first ionization of different monatomic species. In the absence of  $O_2$  in the mixture, the magnitude of the peak at 2.5 kK is significantly higher for 20% compared to 10%  $C_4F_7N$ . Increasing the mole fraction of  $C_4F_7N$  in  $C_4F_7N - CO_2$  mixtures from 10% to 20% results in an increase in the formation of  $CO$  and  $COF_2$  at temperatures below 4 kK. However, with the addition of up to 20%  $O_2$  to these mixtures, the mole fractions of  $CO$  are significantly reduced, while those of  $CO_2$  and  $COF_2$  are increased. With increasing % $O_2$  in the original mixture, the peaks at 3.5 kK for both 10% and 20%  $C_4F_7N$  mixed with  $CO_2$  gain small contributions from the dissociation of  $O_2$ , which can be observed through the tiny peaks on top of the peak in the absence of  $O_2$ . The specific heat results for 10% and 20%  $C_4F_7N$  mixed with  $CO_2$  and without  $O_2$ , at 5 atm have been observed to be in excellent agreement with published data [2].

## 4. Transport properties

The transport properties are calculated using the classical Chapman-Enskog method [6] involving the calculation of collision integrals, which requires primarily as input relevant inter-molecular/atomic potentials for interactions between different species. The neutral-neutral and non-parent neutral-charged species in-

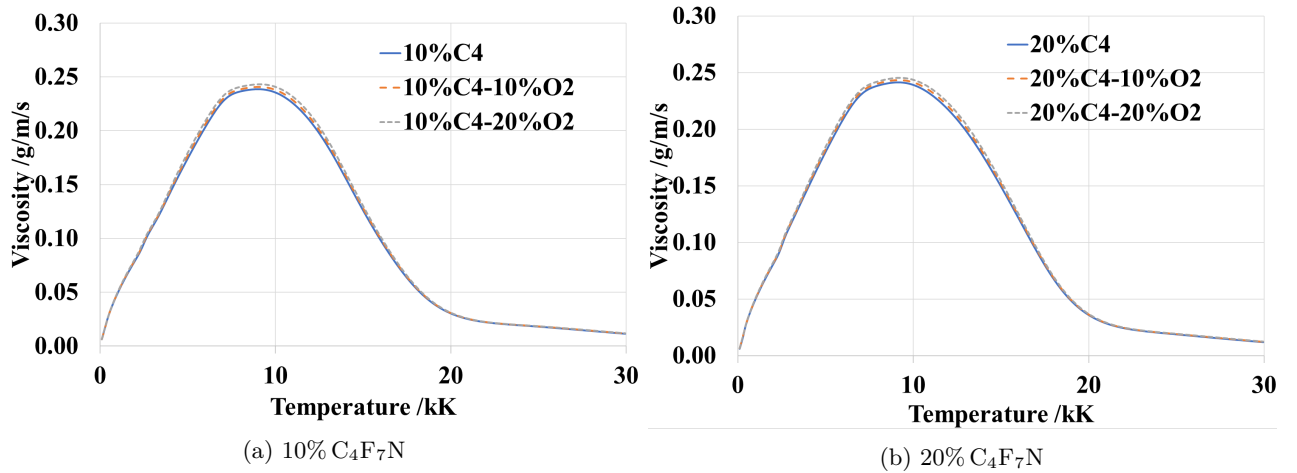


Figure 2. Viscosity values for different  $C_4F_7N$  ( $C_4$ ) mixtures at 1 bar.

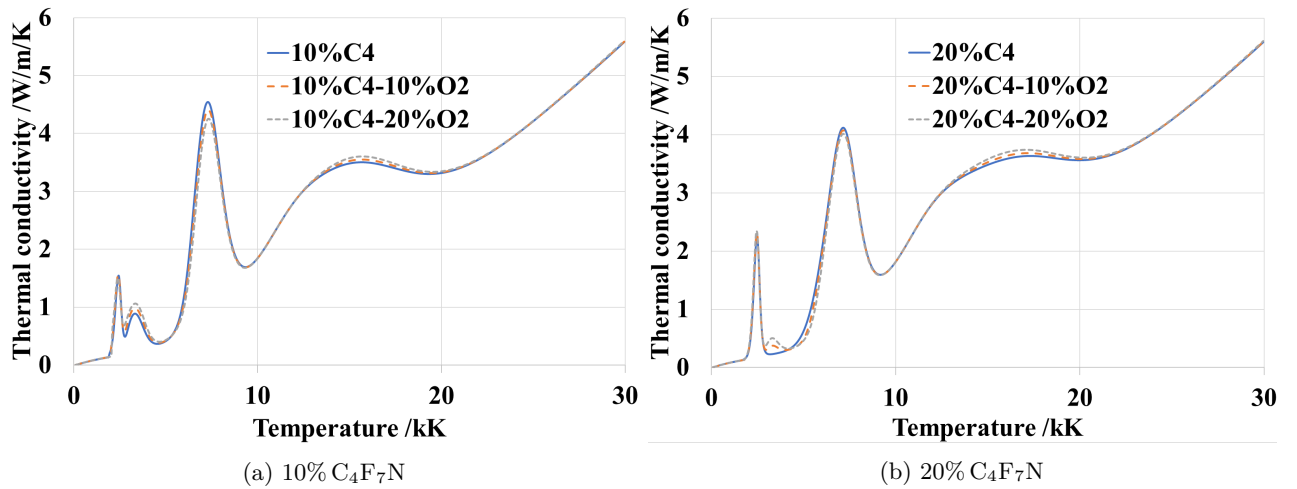


Figure 3. Thermal conductivity values for different  $C_4F_7N$  ( $C_4$ ) mixtures at 1 bar.

interactions are described using the phenomenological Lennard-Jones Potential, which require as input the static polarizabilities and effective electron numbers. For polyatomic species with data unavailable from the literature, the dipole polarizabilities are typically solved via coupled-perturbed Hartree-Fock calculations (used for DFT methods) or using a linear response approximation. According to a benchmark study, both dipole moments and polarizabilities exhibit a slow convergence with the size of the basis set; for aug-cc-pVTZ basis set, the results appear to be converged. We have calculated average polarizability ( $\alpha$ ) and polarizability anisotropy ( $\Delta\alpha$ ) of  $C_4F_7N$  in the gas phase for the global minimum (B3LYP/aug-cc-pVTZ) and along an NVT molecular dynamics (B3LYP/6-31+g\*) trajectory. The parent neutral-charged species interactions are handled using the charge-transfer cross section approximation of the form:  $Q_{ex} = (A - B \ln E)^2$ , where  $E$  is the collisional energy. The charged-charged species interactions are described using the Debye-length based screened Coulomb potential. The Debye-length has been calculated without including the contributions

from ionic species. Finally, the momentum-transfer cross section data available from the literature is utilized for electron-neutral species interactions. The cross-section data for several complex polyatomic species,  $C_4F_7N$  for example, are currently unavailable and have been neglected in our calculations. The assumption is valid since  $C_4F_7N$  dissociates into minor molecular fragments before the appearance of electrons at temperatures greater than 4 kK.

The results for the dynamic viscosity variation with temperature are depicted in figure 2. Neither the temperature at the viscosity peak nor the magnitude of the viscosity peak are significantly altered by increasing either the % $C_4F_7N$  or % $O_2$ . However, we have observed significant differences in the location and the magnitude of the peak, compared to the published data for 10% and 20%  $C_4F_7N - CO_2 - O_2$  mixtures at 5 atm. The temperature at the viscosity peak and the peak viscosity magnitude from our work are approximately: 9.6 kK and 0.24 mPa-s respectively, while these values from published data are approximately: 15 kK and 0.175 mPa-s respectively. The reasons for these discrepancies are currently under investigation.

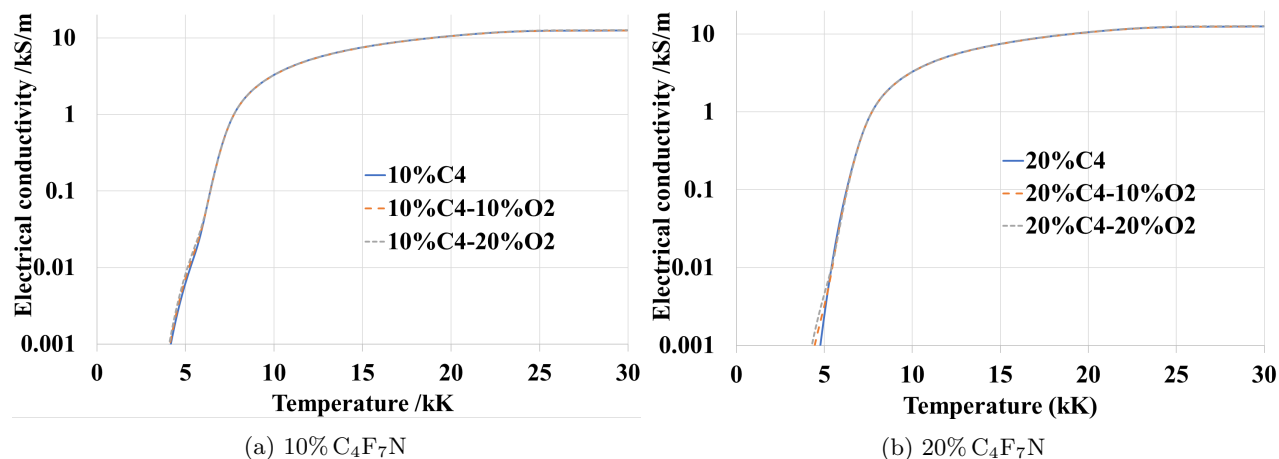


Figure 4. Electrical conductivity values for different  $C_4F_7N$  ( $C_4$ ) mixtures at 1 bar.

Nonetheless, our dynamic viscosity results for pure  $CO_2$  have been observed to be in excellent agreement with those reported in an earlier work [7] compared to those in the recent work [2].

The thermal conductivity results for the different mixtures are plotted in figure 3. It can be clearly observed that the profiles, especially the temperatures corresponding to the different peaks, mirror closely those from the specific heat. The only distinct difference between 10% and 20%  $C_4F_7N - CO_2 - O_2$  mixtures is the significantly higher peak at around 2.6 kK for the latter case compared to the former. This peak is expected to be arising from the dissociation of  $COF_2$  and  $COF_2$  formation is enhanced by increasing the mole fraction of  $C_4F_7N$  from 10% to 20%. Similar to those for the specific heat, the peaks at 3.5 kK are expected to contain contributions from dissociation of  $CO_2$  and  $O_2$ , while the peaks at 7 kK correspond to  $CO$  dissociation. Nonetheless, the maximum relative error between our results with data from the literature [2] for 10% and 20%  $C_4F_7N - CO_2 - O_2$  mixtures at 5 atm is approximately 25%, corresponding to the magnitude of the peak at 7 kK: 4.2 W/m/K calculated vs. 3.2 W/m/K in the published data. This discrepancy is expected to be a consequence of utilization of different interaction potentials corresponding to  $CO$ -related interactions.

The results of electrical conductivity variation with temperature are shown in figure 4. Similar to the dynamic viscosity, there are no significant changes to the electrical conductivity values upon the addition of  $O_2$ . Moreover, the results for 10% and 20%  $C_4F_7N$  mixed with  $CO_2$  at 5 atm are in excellent agreement with published data [2].

## 5. Conclusions

The calculation of thermodynamic and transport properties are necessary for analyzing the performance of promising  $SF_6$  alternatives as an arc switching medium within medium voltage switchgear geometries. In this contribution, these properties have been

calculated for two specific  $C_4F_7N - CO_2$  gas mixtures, with 10% and 20%  $C_4F_7N$  together with the addition of up to 20%  $O_2$ . Based on the equilibrium chemical composition results, increase in the % $C_4F_7N$  results in an increase in the formation of  $CO$ . Even though the addition of  $O_2$  results in significant reduction in the formation of  $CO$ , it enhances the production of  $COF_2$ .

## Acknowledgements

This work is part of the project Nr. TH03020063 of the Technological Agency of the Czech Republic.

## References

- [1] H. Nechmi et al. Fluoronitriles/ $CO_2$  gas mixture as promising substitute to  $SF_6$  for insulation in high voltage applications. *IEEE Trans. Dielectr. Electr. Insul.*, 23(5):2587–2593, 2016. doi:10.1109/TDEI.2016.7736816.
- [2] Y. Wu et al. Properties of  $C_4F_7N-CO_2$  thermal plasmas: thermodynamic properties, transport coefficients and emission coefficients. *Journal of Physics D: Applied Physics*, 51(15):1552061–12, 2018. doi:10.1088/1361-6463/aab421.
- [3] G. Petersson et al. A complete basis set model chemistry. I. The total energies of closed-shell atoms and hydrides of the first-row atoms. *J. Chem. Phys.*, 89(4):2193–218, 1988. doi:10.1063/1.455064.
- [4] L. Curtiss et al. Gaussian-4 theory. *J. Chem. Phys.*, 126(8):0841081–12, 2007. doi:10.1063/1.2436888.
- [5] G. Godin and Y. Trepanier. A robust and efficient method for the computation of equilibrium composition in gaseous mixtures. *Plasma Chem Plasma Process.*, 24(3):447–473, 2004. doi:10.1007/s11090-004-2279-8.
- [6] S. Chapman and T. Cowling. *The mathematical theory of non-uniform gases*. Third edition. John Wiley Inc., 1970.
- [7] A. Yang et al. Thermodynamic properties and transport coefficients of  $CO_2-Cu$  thermal plasmas. *Plasma Chem Plasma Process.*, 36(4):1141–1160, 2016. doi:10.1007/s11090-016-9709-2.